PHYSICAL REVIEW B
CONDENSED MATTER

THIRD SERIES, VOLUME 44, NUMBER 10 1 SEPTEMBER 1991-II

Energy transfer from noble-gas ions to surfaces: Collisions with carbon, silicon, copper, silver, and gold in the range 100–4000 eV

H. Coufal, Harold F. Winters, and H. L. Bay*
IBM Research Division, Almaden Research Center, 650 Harry Road, San Jose, California 95120-6099

W. Eckstein
Institut für Plasmaphysik, D-8046 Garching, Federal Republic of Germany
(Received 11 December 1990)

The energy deposited into carbon, silicon, copper, silver, and gold surfaces by He^+, Ar^+, and Xe^+ ions impinging with kinetic energy in the range 100–4000 eV has been measured. These studies employed a highly sensitive calorimeter together with a modified physical electronics instrument ion gun. Pulses of ions from the gun were directed at the film that had been evaporated directly onto the pyroelectric material. A voltage proportional to the energy deposited is developed across the material and sensed with a lock-in detector. Xe^+ deposits more than 95% of its energy between 500 and 4000 eV for all materials. The other ions deposit at least 80% of their energy in this range. The dependence of energy deposition upon ion and substrate mass and ion energy is about that expected from calculations and physical principles. The energy reflection from surfaces is also investigated by computer simulation using the TRIM.SP program. The experimental trends are semiquantitatively reproduced by the simulation, but there are some quantitative differences in the absolute results. As would be expected from previous calculations, the energy-reflection coefficients do not appear to scale with the ratio of target mass to ion mass or with reduced energy. The implication of these results for the understanding of collisional processes at solid surfaces will be discussed.

I. INTRODUCTION

Knowledge of the amount of energy that an incoming atom or ion transfers to a surface during a collision is essential for the accurate modeling of many technologically important processes, including sputtering, plasma etching, and ion implantation.[1,2] It is also crucial to the design of thermonuclear fusion reactors where energy losses from the plasma to the reactor walls have important consequences for the particle and energy balance of the system.[3]

The efficiency of energy transfer can be described semiquantitatively in terms of the energy-reflection coefficient $R(E)$, the mean value of the fraction of the incident energy E reflected from the surface, or, equivalently, in terms of the energy deposition coefficient $F(E)\equiv[1-R(E)]$. This quantity is expected to be a function of the mass, kinetic energy, and angle of the incident species, as well as the mass of the substrate atoms and possibly the surface morphology. Theoretical expressions and phenomenological descriptions for $R(E)$ remain untested because of an almost complete absence of relevant experimental measurements below a few keV. In part this is due to the considerable experimental difficulties associated with these measurements, particularly at low energies.

In this paper we report results of a systematic study of energy deposition from normally incident, singly charged noble-gas ions to surfaces. We have employed a novel pyroelectric calorimeter to measure the fractional energy deposition $F(E)$ for He, Ar, and Xe ions striking carbon, silicon, copper, silver, and gold surfaces at energies in the range 100–4000 eV. The criteria for choosing target materials was their atomic weight and their ability to remain free of contamination under ion bombardment and ultrahigh-vacuum conditions.

There have been a number of previous studies of energy deposition for ions with energies above 3500 eV (Refs. 4–9) and a range of theoretical calculations and simulations.[10–13] However, there has been little work at low ion energies. Early work by Winters[14] was difficult to interpret as measurements were made with a poorly defined incidence angle. Similarly, the results of Gesang, Oechsner, and Schoof[15] were taken in a plasma environment where accurate current measurements are difficult to

make. Eckstein and Verbeek[16] and Sorensen[17] have published some results for energies down to 1.5 keV, but these are restricted to the case of protons. More recently, Winters *et al.* investigated the energy deposition into gold and platinum in the range between 1 and 4000 eV with helium, argon, and xenon ions.[1] There have also been several reviews of the subject.[18–22]

The first theoretical estimates of the reflection coefficients were derived by Sigmund, who showed that it was possible analytically to calculate the energy contained in the tail of the collision cascade which extends through the surface.[10] He considered the relative amount of energy reflected from the surface,

$$R(E)=E_{\text{out}}/E_{\text{in}} ,$$

when ions of mass M_1 are incident on target atoms of mass M_2, and coined the term "sputtering efficiency" for this parameter, which is called the "energy reflection coefficient" in the present paper. Sigmund's calculations indicated the general size of $R(E)$, that it was independent of incident ion energy above about 1 keV, that the reflected ion (neutral) carried away a significant amount of energy for large values of M_2/M_1, and that $R(E)$ is a function of M_2/M_1, i.e., that it depends upon the ion-target combination only through the mass ratio. Certain aspects of this theory do not quantitatively agree with experimental data; some dependence on incident energy and M_2/M_1 is typically observed in experiments. The predicted trends are, however, substantiated at low energies by the present work and at larger incident energies by previous investigations.

Eckstein and Biersack have investigated the backscattering of heavy ions from surfaces by computer simulation using a binary collision model and the TRIM.SP program.[12] They showed that the particle and energy-reflection coefficients scale with the ratio M_2/M_1 and with a reduced energy ε for $\varepsilon > 0.02$ at normal incidence. They found that at lower energies the scaling breaks down. The reduced energy ε is defined by

$$\varepsilon = aM_2E_{\text{in}}/[Z_1Z_2e^2(M_1+M_2)] ,$$

where Z_1 and Z_2 are the charge of the incident and target ions and a the Firsov screening length for the collision, $a = 0.8853a_0(Z_1^{1/2}+Z_2^{1/2})^{-2/3}$, with a_0 being the Bohr radius.

II. EXPERIMENTAL

The apparatus has been previously described in detail[1] and therefore it will only be reviewed briefly in this section. The relevant experiments are conceptually simple. We wish to measure the fraction of the incident energy that is deposited into the solid. This requires preparation of ions of a known energy which can be directed at a target surface, the quantitative detection of the amount of energy deposited, and the number of ions striking the surface.

A commercial ion gun (PHI 20-115), which was used for all measurements, is shown schematically in Fig. 1. For this work the associated electronics were modified so

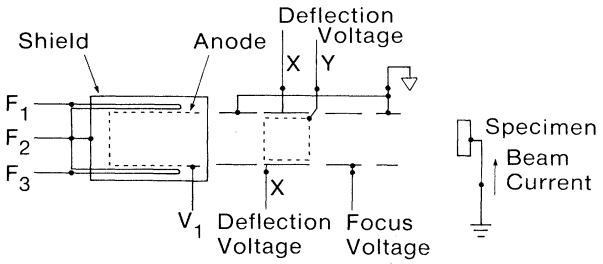

FIG. 1. Schematic diagram of a PHI (20-115) ion gun. V_1 and V_2 are potentials with respect to the ground. F_1 and F_2 are filaments.

that the focus voltage and the voltages which control the ion and electron energies could be varied continuously. Custom electronics were used to apply a 3-Hz modulation voltage to the x deflection plates in order to produce at the sample under study an ion beam with a square-wave time dependence. The ion energy remains well defined because the ions are generated and extracted from a field-free region. The ions are singly charged because the electron energy (the potential difference between the cathode and anode) is maintained below the level that would be needed to generate the doubly charged species. This has been experimentally verified by focusing the beam into a quadrupole mass spectrometer which showed no appreciable intensity at mass peaks due to doubly charged ions. Using the same technique, it was also established that ions from impurity gases had negligibly small intensity.

In Fig. 2 the ion current to the collector surface is shown as a function of the potential difference between the ion gun anode (see Fig. 1) and the collector. The decrease in ion current near zero potential difference occurs because not all of the ions have enough energy to reach the collector surface. The curve shows that the ion energy in eV is 8 V less than V_1 (see Fig. 1) and that the energy spread is approximately 3–4 eV.

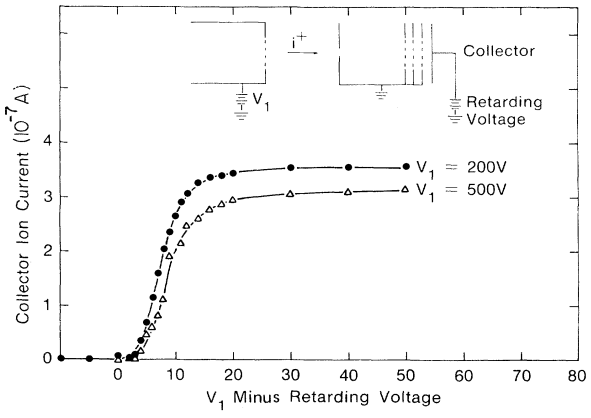

FIG. 2. Current to collector vs V_1 minus the retarding voltage.

Calibration procedures and a detailed description of the calorimeter have been previously published,[1,23] and therefore only a brief account will be given here. Measurements are typically made with an ion-beam modulation frequency of 1–3 Hz. The energy input due to the ion beam striking the grounded surface produces a modulated heating of the pyroelectric calorimeter, which induces a voltage at the calorimeter's back surface. This modulated voltage is detected using lock-in techniques. The output voltage is linearly proportional to the energy input, as indicated by the observation that the output signal is linear with ion-bombardment current under all conditions (see Fig. 3). The intercept of the signal-versus-current curve is close to zero at all ion energies.

The calibration of the calorimeter was established in two independent ways. In the first, the calorimeter surface was illuminated with a ~1-mW He-Ne laser where the needed absorption coefficient was ascertained from reflectivity measurements. The laser power was chosen such that the laser-induced temperature modulation was of the same magnitude as the ion-beam-induced heating to eliminate all errors due to any conceivable nonlinear response of the calorimeter. The absolute laser power was then determined with a NBS-traceable thermopile. Then the laser beam was modulated with a mechanical chopper to obtain full modulation of the laser. By adjusting rotational speed of the mechanical chopper such that the beat frequency between ion-beam modulator and modulated laser beam was zero within experimental error, we ensured that modulation frequency and all overtones during the calibration were identical to those during the other experiments. This is crucial because of the $1/f$ frequency dependence of the observed signal and nonideal response of lock-in amplifiers.[23] The calibration was, therefore, performed under conditions that are identical to those of the ion-beam experiments and is estimated to be accurate within 5%. A second method is based on the measurement of the amount of energy transferred from a 4000-eV singly charged xenon-ion beam to a carbon film, for which we assume that the deposition coefficient $F(E)$ is 0.99. This value was demonstrated within experimental error to be independent of energy between about 500 and 4000 eV, and therefore calibrations could be performed over this entire range, although it was typically done at 4000 eV. These two calibrations agree to within their mutual uncertainties.

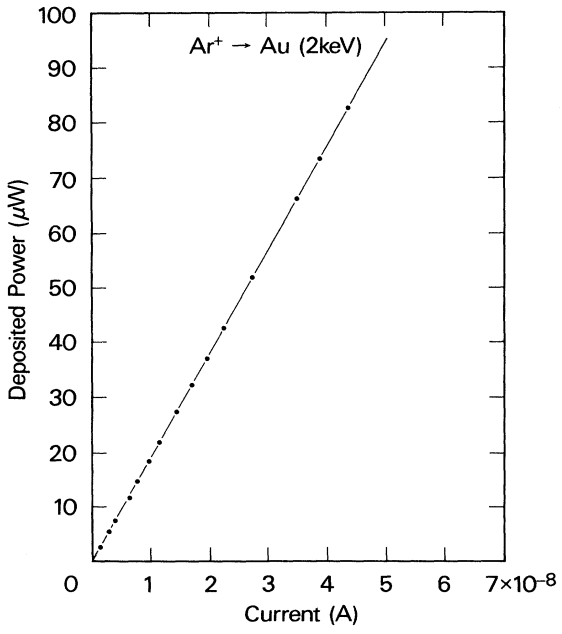

FIG. 3. Deposited energy vs ion current to calorimeter.

All data reported here have been referenced to scale factors determined by the latter method with $F(E)$ taken to be 0.99. The fact that carbon has a small mass, a very small sputter yield, and a small secondary-electron coefficient makes it reasonable to assume that virtually all of the incident energy is deposited into the substrate; hence, the assumption of 0.99. We estimate that this calibration has a possible uncertainty of a few percent. Calibration was accomplished routinely at the conclusion of the experiments with a given sample by depositing carbon onto the film and bombarding the detector with a 3–4-keV Xe^+ beam of well-defined intensity and ion energy. At first, carbon layers were deposited by magnetron sputtering. However, it was soon discovered that carbon (with some hydrogen) which was deposited by bombardment with methane ions produced the same results. Therefore, after measurements for a given substrate material was completed, a carbon layer was deposited using methane ions and the calibration factor determined. A typical value was 15.7 V/W.

The primary uncertainty of the results is related to the calibration. If in the future it is determined that $F(E)$ for 4000-eV Xe^+ on carbon is slightly different from 0.99, then the entire set of data can be corrected. The data taken on the same calorimeter are extremely reproducible. Hence the relative values for $F(E)$ as a function of ion energy and mass should be accurate to better than 2%. Measurements were made on three different calorimeters for gold and copper and on two different calorimeters for silver. When all the data from all calorimeters obtained under equivalent conditions (same ion mass and energy, 5–25 independent measurements) are averaged, the standard deviation is typically 1%–2% of the mean. This implies that when the differences from sample to sample, the changes in surface condition with fluence, and the reproducibility of the measurements are taken into account, there is an estimated uncertainty of less than 2%. The uncertainty in the calibration must be added to this estimate.

It is conceivable that a fraction of a monolayer of a light adsorbate could influence energy transfer to the high-mass substrates. It was therefore important to estimate surface contamination levels. The electron beam needed to perform Auger spectroscopy destroyed several calorimeters because of overheating and/or arcing resulting in the loss of the calorimeter prior to calibration. In this context it is important to remember that the calorimeter was designed such that a minimum heat input effects a maximum temperature increase. This can lead to a

temperature increase above the Curie temperature of the pyroelectric where it is depolarized. In addition, a material with a very large pyroelectric figure of merit was selected, ensuring that the temperature increase causes a maximum signal voltage across the sensor element. Because of the fact that the calorimeter is only several μm thick, to minimize lateral heat loss in the device, even a relatively small voltage can lead to electric fields above the breakdown field of the pyroelectric. Therefore, routine Auger analysis was not performed during an experiment. However, Auger spectra were taken after the data had been accumulated under conditions which were considered to be typical. Auger spectra for gold were shown in a previous publication.[1] Typical examples for copper and silver are shown in Fig. 4. The surface is clean except for a small carbon peak, from which we estimate an upper limit for carbon coverage of a few percent of a monolayer. Auger spectra for carbon and silicon films on the calorimeter were not successfully obtained. However, data taken on control samples in another vacuum system with a poorer ultimate pressure indicate that the carbon is atomically clean. Similar data for silicon indicate some oxygen and a small quantity of argon. The amplitude of the silicon Auger peak is at least 7 times that of the oxygen. Examination of the Auger spectra between 70 and 100 eV showed little or no evidence for silicon dioxide. It is possible that the oxygen which was observed was incorporated into the film during deposition.

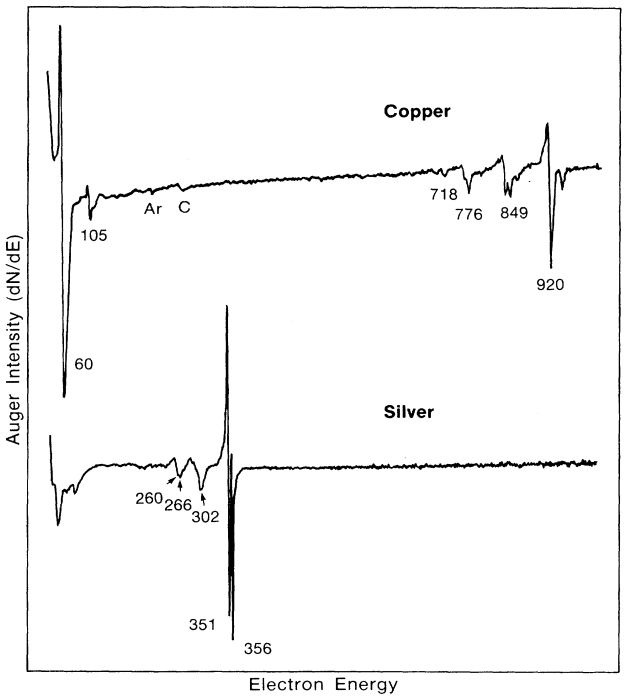

FIG. 4. Auger spectrum for the evaporated copper and silver films deposited on the calorimeter surface. The conditions are believed to be typical of those existing during energy deposition experiments. Substrate peaks are designated by their characteristic energy. Carbon is indicated by a C.

The pressure in the vacuum system was always less than 3×10^{-10} Torr prior to the experiments. During the experiment, the noble-gas pressure was about 1×10^{-5} Torr.

III. COMPUTATIONAL METHOD

For the calculations we used the Monte Carlo program TRIM.SP, which is described in detail in Ref. 12. The program is based on the binary-collision model and uses a randomized target structure. Weak collisions with large impact parameters are taken into account as simultaneous collisions. This is an approximate way to account for interactions with more than one atom at a collision site. The krypton-carbon interaction potential was used.[24] This potential has been shown to be a good average for most ion-target combinations.[25] For the inelastic energy loss, we applied a 50%-50% contribution of a nonlocal loss according to Lindhard and Scharff[26] and a local loss due to Oen and Robinson.[27] The inelastic stopping data from Ziegler's tables[28] were used for He. For the noble gases we used a cutoff energy of E_F equal to 0.5 eV and a surface binding energy of zero. For sputtered particles a planar surface potential was assumed with a surface binding energy as designated in Tables I–V. For comparison of calculations with experiment it should be assumed that the calculated values for $R(E)$ have a statistical uncertainty of less than a few percent, but the systematic uncertainty may be larger than 20%.

IV. RESULTS

A. Carbon

The fraction energy deposited into carbon for He^+, Ar^+, and Xe^+ in the energy range between 100 and 4000 eV is shown in Fig. 5. Data along with calculated results are tabulated in Table I. Helium, argon, and xenon transfer most (98%) of their energy to the lattice in the range between 500 and 4000 eV. Both, calculations and experiment, indicate that the ion masses do not have much influence on the amount of energy carried away by the reflected ion (neutral) when the target-mass--to–ion-

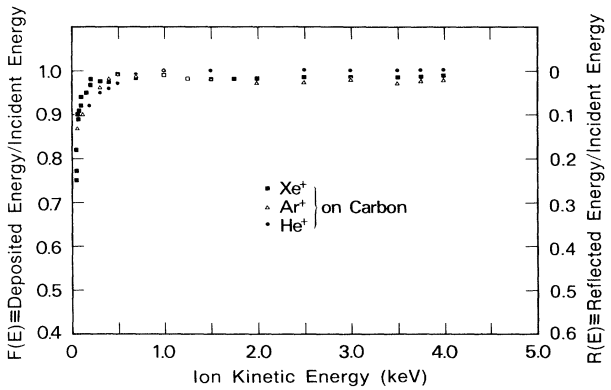

FIG. 5. Fraction of the incident energy of Xe^+, Ar^+, and He^+ deposited in carbon for normal incidence at ion energies up to 4000 eV.

TABLE I. Energy deposited into carbon. $F(E)$=fraction of energy deposited by ion, $R(E)=1-F(E)$, $R(I)$=fraction of energy carried away by reflected ion (neutral), $Y(E)$=fraction of energy carried away by sputtered particles, Y=sputter yield, and $U_s=7.40$ eV.

	Energy	$F(E)_{\text{expt}}$	$F(E)_{\text{TRIM}}$	$R(E)$	TRIM $Y(E)$	$R(I)$	Y
He→C							
	4000	1.0	0.995	4.53×10^{-3}	3.45×10^{-4}	4.18×10^{-3}	4.08×10^{-2}
	1000	1.0	0.986	1.36×10^{-2}	1.29×10^{-3}	1.23×10^{-2}	5.44×10^{-2}
	500	0.97	0.981	1.89×10^{-2}	1.79×10^{-3}	1.71×10^{-2}	5.21×10^{-2}
	300	0.95	0.976	2.40×10^{-2}	2.05×10^{-3}	2.19×10^{-2}	4.62×10^{-2}
	100		0.965	3.52×10^{-2}	1.43×10^{-3}	3.38×10^{-2}	2.06×10^{-2}
Ar→C							
	4000	0.98	0.995	4.95×10^{-3}	4.95×10^{-3}	0	6.32×10^{-1}
	1000	1.0	0.996	4.09×10^{-3}	4.09×10^{-3}	0	2.64×10^{-1}
	500	0.99	0.998	2.55×10^{-3}	2.55×10^{-3}	0	1.23×10^{-1}
	300	0.96	0.999	1.24×10^{-3}	1.24×10^{-3}	0	4.96×10^{-2}
	100	0.90	1.00	2.27×10^{-5}	2.27×10^{-5}	0	7.35×10^{-4}
Xe→C							
	4000	0.99	0.997	3.10×10^{-3}	3.10×10^{-3}	0	5.99×10^{-1}
	1000	0.99	0.999	1.20×10^{-3}	1.20×10^{-3}	0	1.28×10^{-1}
	500	0.99	1.00	3.47×10^{-4}	3.47×10^{-4}	0	3.00×10^{-2}
	300	0.97	1.00	5.22×10^{-5}	5.21×10^{-5}	0	3.89×10^{-3}
	100	0.93	1.00	1.74×10^{-6}	0	0	0

mass ratio is less than 3. The main influence of ion mass for this small ratio is to change the quantity of energy carried away by sputtered particles. For carbon the sputter yield is small, and hence this contribution is always less than 1% (see Table I).

Below about 500 eV the experiment shows that the deposited energy decreases, while calculations indicate it to be constant for argon and xenon and to decrease slightly for helium. In any case the agreement between theory and experiment is reasonably good for carbon.

The use of the PHI ion gun for energies below about 200 eV leads to more uncertainty in the results than is present at higher energies. Hence the sharp decrease in $F(E)$ shown in Fig. 5 at energies below 100 eV is suggestive, but needs to be verified with a better defined ion beam such as that described in Ref. 1.

B. Silicon

Figure 6 shows the fractional energy deposited into silicon for He^+, Ar^+, and Xe^+ in the energy range between 200 and 4000 eV. Data along with calculated results are tabulated in Table II. Argon and xenon transfer most (98%) of their energy to the lattice in the range between 700 and 4000 eV. At smaller energies, $F(E)$ increases from about 0.98 to 1.00 for xenon and decreases for argon and helium.

The agreement between experiment and theory is quite good for xenon at all energies and for the other gases at 4000 eV. Table II shows that at lower energies argon deposits less energy than predicted. For example, at 300 eV, $F(E)$ is predicted to be 0.99 and is observed to be 0.95. The data are even more striking for helium. Both theory and experiment indicate that $F(E)$ will become smaller with decreasing energy, but the decrease which is observed experimentally is greater than predicted. For example, at 300 eV the predicted value is 0.90 and the experimental value is 0.76 (see Table II).

C. Copper

Figure 7 shows the fractional energy deposited into copper for He^+, Ar^+, and Xe^+ in the energy range between roughly 100 and 4000 eV. Data along with calculated results are tabulated in Table III. The points in Fig. 7 and the data in Table III are unweighted averages of measurements taken on three different calorimeters. The mean value for the standard deviation calculated for all

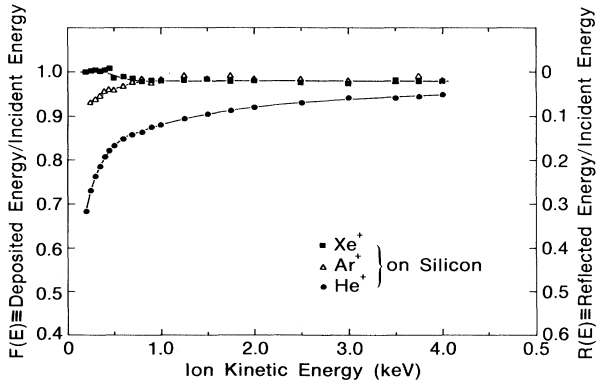

FIG. 6. Fraction of the incident energy of Xe^+, Ar^+, and He^+ deposited in silicon for normal incidence at ion energies up to 4000 eV.

TABLE II. Energy deposited into silicon. $F(E)$=fraction of energy deposited by ion, $R(E)=1-F(E)$, $R(I)$=fraction of energy carried away by reflected ion (neutral), $Y(E)$=fraction of energy carried away by sputtered particles, Y=sputter yield, and $U_s=4.70$ eV.

	Energy	$F(E)_{\text{expt}}$	$F(E)_{\text{TRIM}}$	$R(E)$	TRIM $Y(E)$	$R(I)$	Y
He→Si							
	4000	0.949	0.966	3.38×10^{-2}	6.47×10^{-4}	3.32×10^{-2}	8.00×10^{-2}
	1000	0.88	0.931	6.88×10^{-2}	1.99×10^{-3}	6.68×10^{-2}	1.04×10^{-1}
	500	0.83	0.913	8.66×10^{-2}	2.88×10^{-3}	8.37×10^{-2}	1.01×10^{-1}
	300	0.765	0.901	9.88×10^{-2}	3.37×10^{-3}	9.54×10^{-2}	8.77×10^{-2}
	100		0.873	1.27×10^{-1}	2.61×10^{-3}	1.24×10^{-1}	4.43×10^{-2}
Ar→Si							
	4000	0.98	0.992	8.63×10^{-3}	8.34×10^{-3}	1.68×10^{-5}	1.19
	1000	0.98	0.991	9.34×10^{-3}	9.26×10^{-3}	7.64×10^{-5}	0.66
	500	0.959	0.992	7.64×10^{-3}	7.58×10^{-3}	6.04×10^{-5}	0.40
	300	0.946	0.994	5.73×10^{-3}	5.65×10^{-3}	8.09×10^{-5}	0.23
	100		0.999	1.17×10^{-3}	1.10×10^{-3}	7.12×10^{-5}	0.031
Xe→Si							
	4000	0.98	0.992	7.87×10^{-3}	7.87×10^{-3}	0	1.48
	1000	0.98	0.994	5.98×10^{-3}	5.98×10^{-3}	0	0.55
	500	0.985	0.996	3.87×10^{-3}	3.87×10^{-3}	0	0.26
	300	1.004	0.998	2.09×10^{-3}	2.09×10^{-3}	0	0.11
	100		1.00	9.38×10^{-5}	9.24×10^{-5}	0	3.48×10^{-3}

measurements of $F(E)$ at a given energy is 0.0175. $F(E)$ for argon and xenon are equal within experimental error at high energy and diverge slightly below 500 eV. Above about 750 eV roughly 98% of the energy is deposited into the lattice. At smaller energies $F(E)$ decreases somewhat, but is generally above 0.9. $F(E)$ for helium is 0.91 at 4000 eV and decreases to about 0.82 at 300 eV.

There are only a few sources of data in the literature which can be compared with the present work. These include Koborov *et al.*[7] who measured $R(E)$ for He^+ on copper at 4 keV and obtained a value of about 0.09, which is identical to the results obtained in the present work (see Table III). Furthermore, extrapolation of the work of Schou, Sorensen, and Littmark from 5 to 4 keV gives about the same value.[5] Moreover, Oen and Robinson have calculated the energy reflection from copper in the energy range between 10 and 20 keV using the binary-collision cascade simulation program MARLOWE.[13] There is good agreement between our experimental results and their calculated values over the entire energy range. The agreement between these investigations and the present work gives confidence in the reliability of the data.

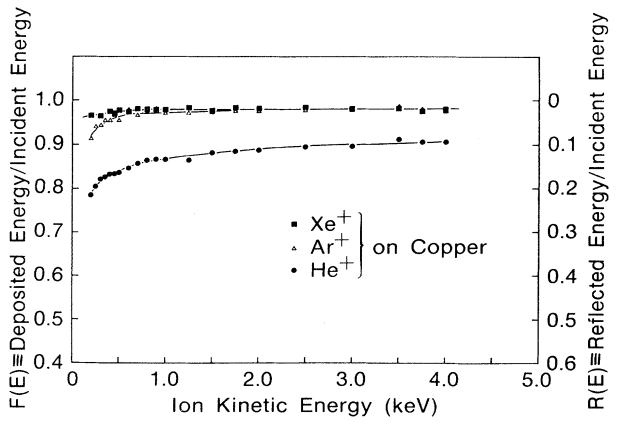

FIG. 7. Fraction of the incident energy of Xe^+, Ar^+, and He^+ deposited in copper for normal incidence and ion energies up to 4000 eV.

The agreement between our experiment and TRIM.SP calculations (see Table III) is excellent at 4000 eV and reasonable at all energies. However, the experimental values for argon and xenon tend to decease faster than the theory would suggest. The opposite is true for helium. The calculations indicate that the reflected energy $R(E)$ is dominated by sputtered particles for argon and xenon and by reflected energetic ions (neutrals) for helium.

D. Silver

The fractional energy deposited into silver for He^+, Ar^+, and Xe^+ in the energy range between roughly 100 and 4000 eV is shown in Fig. 8. Data along with calculated results are tabulated in Table IV. The data points in Fig. 8 and Table IV are averages of several experiments taken on two different calorimeters. $F(E)$ for argon and xenon are equal within experimental error above 1500 eV and diverge below this energy. $F(E)$ tends to decrease with decreasing incident energy for all three gases. The relative magnitude of the decrease is of course largest for helium and smallest for xenon with argon being intermediate. At 4000 eV xenon deposits 98% of its

TABLE III. Energy deposited into copper. $F(E)$=fraction of energy deposited by ion, $R(E)=1-F(E)$, $R(I)$=fraction of energy carried away by reflected ion (neutral), $Y(E)$=fraction of energy carried away by sputtered particles, Y=sputter yield, and $U_s=3.52$ eV.

	Energy	$F(E)_{\text{expt}}$	$F(E)_{\text{TRIM}}$	$R(E)$	TRIM $Y(E)$	$R(I)$	Y
He→Cu							
	4000	0.905	0.90	9.74×10^{-2}	8.52×10^{-4}	9.66×10^{-2}	1.92×10^{-1}
	1000	0.867	0.83	1.66×10^{-1}	2.48×10^{-3}	1.64×10^{-1}	2.13×10^{-1}
	500	0.837	0.81	1.93×10^{-1}	3.49×10^{-3}	1.90×10^{-1}	1.91×10^{-1}
	300	0.821	0.785	2.15×10^{-1}	3.88×10^{-3}	2.11×10^{-1}	1.60×10^{-1}
	100	0.70	0.73	2.71×10^{-1}	2.87×10^{-3}	2.68×10^{-1}	7.77×10^{-2}
Ar→Cu							
	4000	0.977	0.976	2.35×10^{-2}	1.85×10^{-2}	5.01×10^{-3}	3.5
	1000	0.972	0.963	3.68×10^{-2}	2.85×10^{-2}	8.62×10^{-3}	2.27
	500	0.954	0.959	4.14×10^{-2}	3.03×10^{-2}	1.11×10^{-2}	1.55
	300	0.941	0.958	4.19×10^{-2}	2.87×10^{-2}	1.32×10^{-2}	1.05
	100	0.90	0.968	3.19×10^{-2}	1.34×10^{-2}	1.85×10^{-2}	0.265
Xe→Cu							
	4000	0.978	0.98	1.97×10^{-2}	1.97×10^{-2}	0	4.15
	1000	0.976	0.978	2.19×10^{-2}	2.19×10^{-2}	0	2.13
	500	0.978	0.982	1.80×10^{-2}	1.80×10^{-2}	0	1.17
	300	0.964	0.987	1.32×10^{-2}	1.32×10^{-2}	0	0.65
	100	0.96	0.997	2.79×10^{-3}	2.79×10^{-3}	0	0.089

energy into the lattice. This value drops to 96% at 500 eV. The corresponding values at these energies for argon are 97% and 90% and for helium are 89% and 80%, respectively.

Schou, Sorensen, and Littmark[5] have measured the energy-reflection coefficient for helium from silver at 4 keV and obtained a value of 0.13, which is to be compared with the value of 0.115 obtained in the present work. These numbers are equal within experimental uncertainty.

The theoretical and experimental values for the magnitude of $F(E)$ are in reasonable agreement for argon and xenon at most energies (see Table IV). However, in a manner analogous to copper, there is a tendency for the

TABLE IV. Energy deposited into silver. $F(E)$=fraction of energy deposited by ion, $R(E)=1-F(E)$, $R(I)$=fraction of energy carried away by reflected ion (neutral), $Y(E)$= fraction of energy carried away by sputtered particles, Y= sputter yield, and $U_s=2.97$ eV.

	Energy	$F(E)_{\text{expt}}$	$F(E)_{\text{TRIM}}$	$R(E)$	TRIM $Y(E)$	$R(I)$	Y
He→Ag							
	4000	0.885	0.842	1.58×10^{-1}	7.58×10^{-4}	1.57×10^{-1}	0.200
	1000	0.835	0.77	2.30×10^{-1}	1.71×10^{-3}	2.28×10^{-1}	0.182
	500	0.80	0.736	2.64×10^{-1}	2.21×10^{-3}	2.62×10^{-1}	0.151
	300	0.765	0.716	2.84×10^{-1}	2.27×10^{-3}	2.82×10^{-1}	0.120
	100	0.670	0.663	3.37×10^{-1}	1.17×10^{-3}	3.36×10^{-1}	0.043
Ar→Ag							
	4000	0.97	0.95	4.86×10^{-2}	2.38×10^{-2}	2.48×10^{-2}	4.22
	1000	0.94	0.928	7.17×10^{-2}	3.49×10^{-2}	3.68×10^{-2}	2.64
	500	0.90	0.917	8.23×10^{-2}	3.82×10^{-2}	4.41×10^{-2}	1.83
	300	0.85	0.912	8.75×10^{-2}	3.68×10^{-2}	5.07×10^{-2}	1.28
	100	0.68	0.905	9.47×10^{-2}	2.39×10^{-2}	7.08×10^{-2}	0.44
Xe→Ag							
	4000	0.98	0.974	2.61×10^{-2}	2.59×10^{-2}	2.37×10^{-4}	5.79
	1000	0.96	0.97	2.94×10^{-2}	2.91×10^{-2}	2.89×10^{-4}	2.85
	500	0.955	0.973	2.67×10^{-2}	2.63×10^{-2}	3.88×10^{-4}	1.71
	300	0.95	0.979	2.14×10^{-2}	2.11×10^{-2}	3.45×10^{-4}	1.05
	100		0.992	7.64×10^{-3}	6.95×10^{-3}	5.07×10^{-4}	0.21

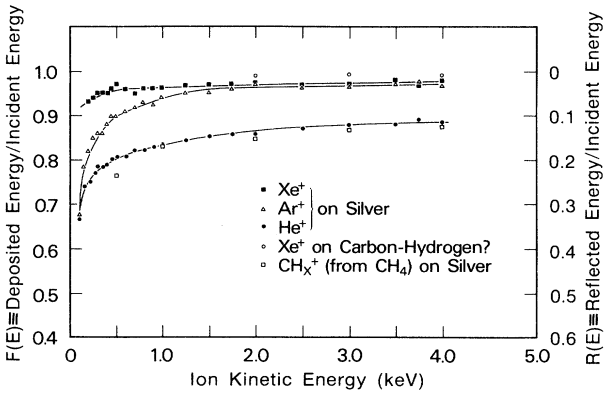

FIG. 8. Fraction of the incident energy of Xe^+, Ar^+, and He^+ deposited in silver for normal incidence and ion energies up to 4000 eV.

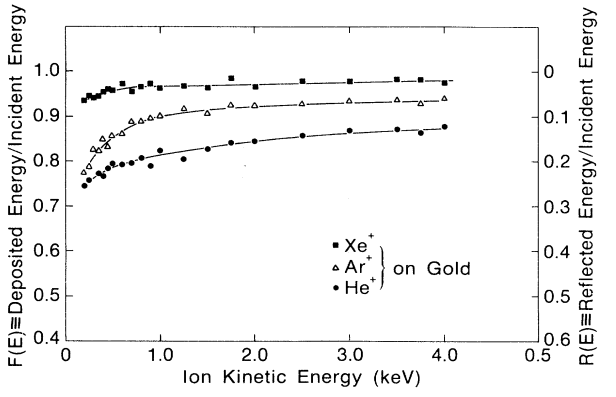

FIG. 9. Fraction of the incident energy of Xe^+, Ar^+, and He^+ deposited in gold for normal incidence and ion energies up to 4000 eV.

experimental values to decrease faster with decreasing energy than do the theoretical ones. In contrast, $F(E)_{\text{expt}}$ for helium is about 0.05 larger than $F(E)_{\text{Trim}}$ at both 4000 eV and 300 eV; i.e., the theoretical and experimental values are slightly different, but the energy dependence is about right. The calculations indicate that most of the reflected energy is carried away by reflected ions (neutrals) for helium. Reflected ions and sputtered particles make roughly equal contributions for argon. In the case of xenon, most of the energy is carried away by sputtered particles.

E. Gold

Figure 9 shows the fractional energy deposited into gold for He^+, Ar^+, and Xe^+ in the energy range between 50 and 4000 eV. Data were taken with two types of ion guns and on several calorimeters. Therefore, the results are believed to be quite reliable. Data along with calculated results are tabulated in Table V. The points in Fig. 9 and the data at 200 eV and above in Table V are unweighted averages of all measurements taken on three different calorimeters. On the average, the standard devi-

TABLE V. Energy deposited into gold. $F(E)$=fraction of energy deposited by ion, $R(E)=1-F(E)$, $R(I)$=, fraction of energy carried away by reflected ion (neutral), $Y(E)$=fraction of energy carried away by sputtered particles, Y=sputter yield, and $U_s=3.80$ eV.

	Energy	$F(E)_{\text{expt}}$	$F(E)_{\text{TRIM}}$	$R(E)$	TRIM $Y(E)$	$R(I)$	Y
He→Au							
	4000	0.87	0.77	2.32×10^{-1}	5.26×10^{-4}	2.31×10^{-1}	0.131
	1000	0.81	0.70	3.03×10^{-1}	9.91×10^{-4}	3.02×10^{-1}	0.106
	500	0.79	0.67	3.34×10^{-1}	9.42×10^{-4}	3.33×10^{-1}	0.0742
	300	0.76	0.64	3.57×10^{-1}	7.63×10^{-4}	3.56×10^{-1}	0.0498
	100	0.71	0.59	4.14×10^{-1}	7.28×10^{-5}	4.14×10^{-1}	5.46×10^{-3}
	50	0.67	0.54	4.56×10^{-1}	0	4.56×10^{-1}	0
Ar→Au							
	4000	0.94	0.89	1.07×10^{-1}	2.60×10^{-2}	8.11×10^{-2}	3.68
	1000	0.90	0.86	1.39×10^{-1}	3.57×10^{-2}	1.03×10^{-1}	2.10
	500	0.85	0.84	1.52×10^{-1}	3.61×10^{-2}	1.16×10^{-1}	1.38
	300	0.81	0.834	1.64×10^{-1}	3.31×10^{-2}	1.31×10^{-1}	0.93
	100	0.73	0.81	1.90×10^{-1}	1.86×10^{-2}	1.71×10^{-1}	0.27
	50	0.67	0.79	2.08×10^{-1}	5.48×10^{-3}	2.02×10^{-1}	7.43×10^{-2}
Xe→Au							
	4000	0.98	0.956	4.42×10^{-2}	3.75×10^{-2}	6.69×10^{-3}	5.95
	1000	0.97	0.95	5.16×10^{-2}	4.14×10^{-2}	1.02×10^{-2}	2.87
	500	0.96	0.95	4.98×10^{-2}	3.77×10^{-2}	1.21×10^{-2}	1.71
	300	0.94	0.956	4.44×10^{-2}	3.11×10^{-2}	1.33×10^{-2}	1.07
	100	0.95	0.973	2.73×10^{-2}	1.07×10^{-2}	1.66×10^{-2}	0.216
	50	0.94	0.981	1.90×10^{-2}	1.73×10^{-3}	1.73×10^{-2}	0.027

ation is 2.0% of the mean value of all measurements for a given energy. Some data for gold has been published previously.[1] Subsequent comparison of gold with other substrates led to the conclusion that the calibration in these experiments was approximately 2% high. This occurred because the measurement with 4000-eV Xe^+ scattering from a gold film, which was used along with a measurement on carbon for calibration, was about 2% too low as is obvious from Fig. 7 of Ref. 1. The data shown in Fig. 9 and Table V have been corrected using the improved, new calibration.

Xenon transfers more than 90% of its energy to the lattice for all ion energies between 100 and 4000 eV. Calculations indicate the same result. However, the experiments indicate that $F(E)$ decreases slightly at lower energies, while the calculations suggest a slight increase. The theory indicates that most of the reflected energy is carried away by sputtered particles. At lower energies the sputter yield and the average energy carried away per sputtered particle become smaller. Hence $F(E)$ becomes larger. This argument is rather convincing. That the experiment shows the opposite trend must originate from the fact that $R(I)$ (the fraction of the incident energy carried away by reflected ions) is larger than calculated for the lower incident energies of the ion.

Argon transfers 67% of its energy to gold at an incident energy of 50 eV and 93% at 4000 eV. The calculated values are 79% and 89% at these energies. The theory is low at high energy and high at low energy. This trend is similar to but larger than that observed for xenon on gold. Gold is the only substrate investigated where the mass ratio is large enough so that $F(E)$ differs significantly between argon and xenon at 4000 eV.

Calculations for helium on gold predict more reflected energy than is observed for all energies. At 4000 eV, TRIM.SP predicts a value for $R(E)$ of 0.23 (see Table V), while a value of 0.13 is observed. At 300 eV the respective values are 0.23 and 0.36.

V. DISCUSSION

This paper presents experimental and numerical data for 15 ion-substrate combinations that are summarized in Fig. 10. As expected, on the basis of the mass ratio, helium on gold has the largest energy-reflection coefficient (0.13) at 4000 eV. At 300 eV the reflection coefficients for gold, silver, and silicon are all similar. The energy transfer generally deceases with decreasing ion energy

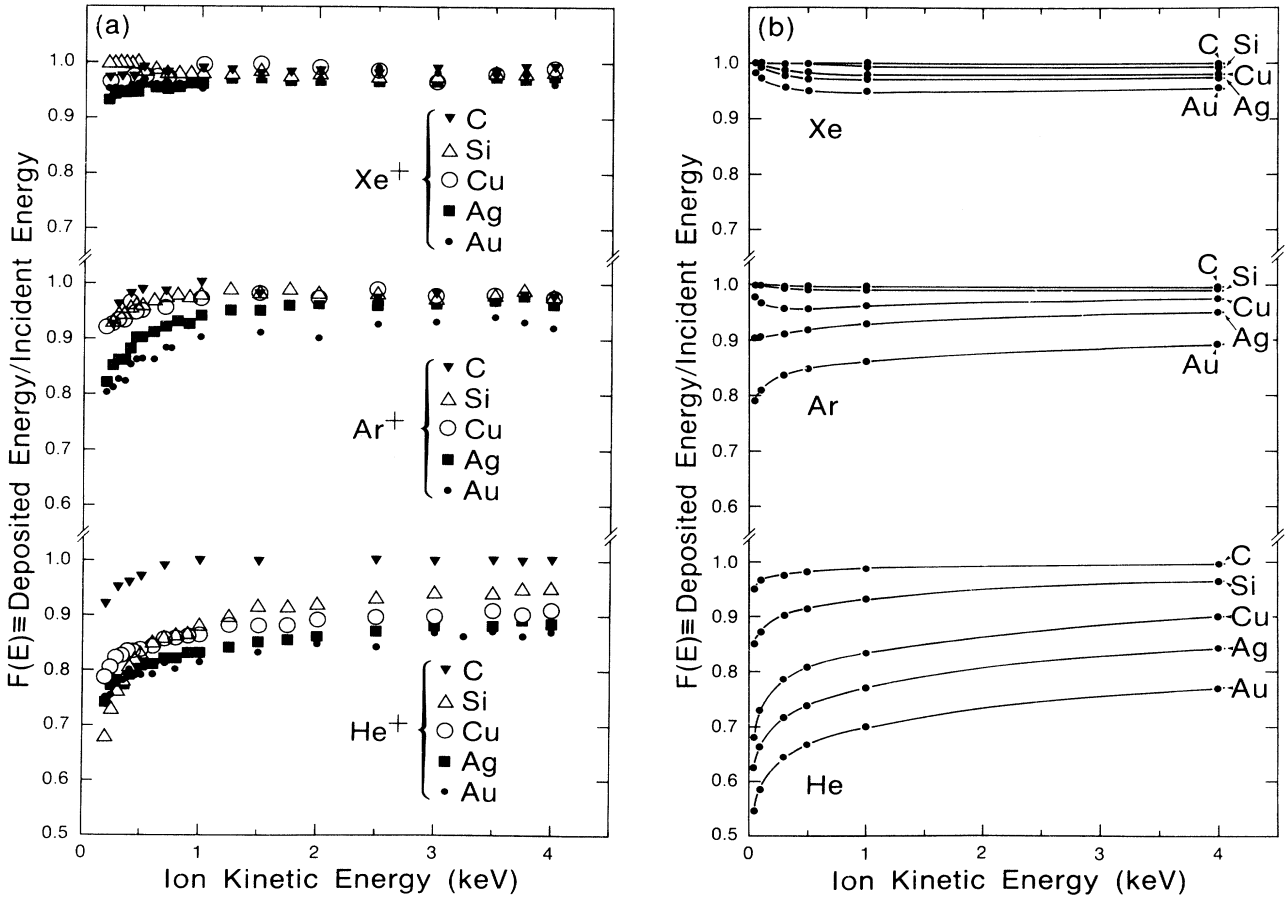

FIG. 10. Fraction of the incident energy of ions deposited into various substrates. On the left side are shown TRIM calculations and on the right side the corresponding experimental data.

and increases with mass ratio. The decrease with ion energy is most pronounced for helium scattered from the silicon samples. Moreover, in contrast to other systems, xenon ions scattered from a silicon substrate exhibit an increase of the energy transfer with decreasing ion energy. Considering the mass ratio, silicon seems to behave somewhat differently at low energy than do the other substrate materials. The ion-energy dependence of the silicon data is, therefore, not typical and might be attributed to sample preparation. A careful characterization of these samples showed, however, no peculiar features for the silicon films other than the slight oxygen content. This should, however, not affect the data appreciably.

Helium transfers the same fraction of its energy to carbon as do xenon and argon over most of the energy range. In contrast, helium transfers a smaller fraction of its energy to silicon. Since the sputter yield is small for helium, most of the reflected energy $R(E)$ is carried away by reflected helium ions (neutrals). Therefore, the carbon-silicon comparison indicates that at the higher energies the reflection of energetic ions becomes important when the mass ratio M_2/M_1 is somewhere between 3 and 7. This conclusion is consistent with all experimental data presented in this paper. At lower energies reflected ions carry away significant energy for even smaller mass ratios.

Eckstein and Biersack have used the TRIM.SP program to check reduced energy scaling of the energy-reflection coefficient $R(E)$ for ion-target combinations with the same mass ratio.[12] Their results suggested that the scaling is fulfilled for $\varepsilon > 0.02$, while for lower incident energies the divergence for different ion-target combinations is increasing. Their conclusion that scaling does not apply at low energies is consistent with our data (see Fig. 11).

Experiments and calculations using the TRIM.SP program agree within their mutual uncertainties for at least one incident ion energy for 14 of the 15 combinations. For He-Au the calculations predict more reflected energy than is observed at all incident energies. Both theory and simulation indicate that the amount of reflected energy increases as the mass ratio M_2/M_1 increases. A similar trend is observed experimentally as shown in Fig. 10. The calculations show that the reflected energy should increase as the incident ion energy decreases. This general trend is also observed in the experimental data. The fact that the calculations correctly predict the trends which are observed experimentally indicates that the TRIM.SP program gives a reasonable description of the physical situation in this energy range.

Nevertheless, there are differences between the calculations and experiment which are outside the range of experimental uncertainty. The deposited energy measured experimentally is estimated to be accurate to 2% for incident energies above 200 eV. This assumes that the calibration with carbon is correct and includes variation from sample to sample, systematic changes with ion dose, and fluctuations from run to run. The reflected energy derived from calculations can change up to 20%, depending upon assumptions. Of the 15 ion-target combinations, calculations and experiment are in reasonable agreement over the entire energy range for five: Xe-Ag, Ar-Cu, Xe-Si, He-C, and Xe-C. The calculations on average predict more reflected energy than is observed for He-Au, He-Ag, and He-Cu. The calculations tend to predict less reflected energy than is observed for Xe-Au, Ar-Ag, Xe-Cu, He-Si, Ar-C, and Ar-Si. In one case, Ar-Au, the Trim calculations give values lower than experiment at high energy and higher than experiment at low energy.

The systems where there is good agreement over the entire energy range tend to be situations where almost all

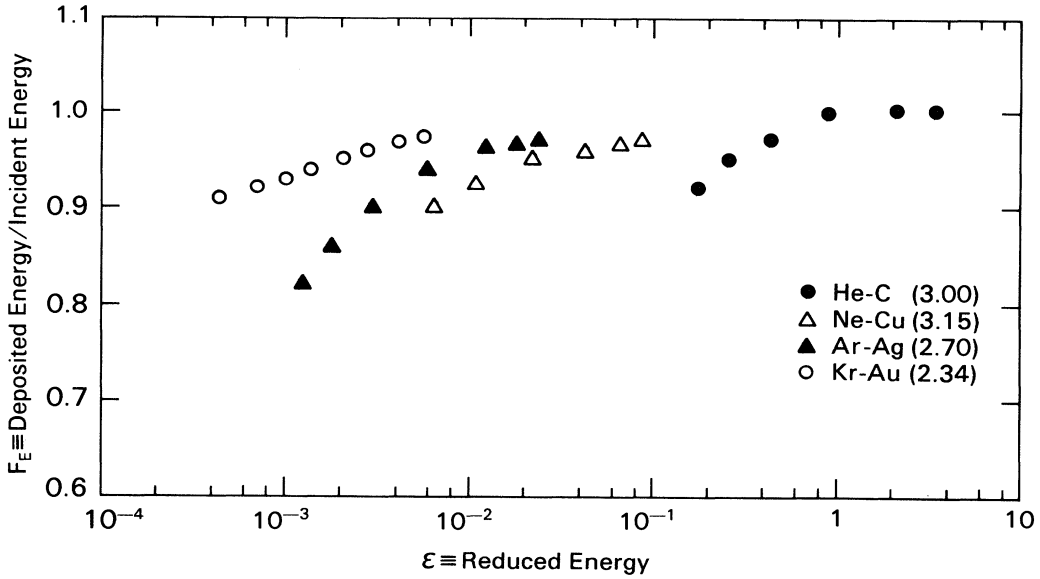

FIG. 11. Relative fraction of energy deposited as a function of the reduced energy ε for four ion-target combinations. The mass ratio M_2/M_1 for each of these combinations is given in parentheses.

the energy is deposited into the lattice. The systems where more reflected energy is predicted than is observed tend to be light ions colliding with heavy substrate materials. When the calculations predict less reflected energy than is observed, the situation is characterized by the fact that there is agreement at high energies where most of the energy is deposited into the lattice and disagreement at lower energies where more is reflected. Even in systems where there is agreement within the experimental uncertainties over the entire energy range, there appears to be a tendency at low incident energies to reflect more energy than predicted. A possible explanation, which has been discussed previously,[1] involves the concept of an effective mass.

It is suspected that the fraction of the collisions which is adequately described by the binary collision approximation slowly decreases as the ion energy becomes smaller. Particles with certain impact parameters may strongly interact with more than one substrate atom at a time. This situation might be described by assuming that the effective mass of the substrate is greater than one atomic mass. The larger effective mass would then lead to more reflected energy than is predicted based upon the binary collision approximation. This mechanism was previously postulated to explain the sharp increase in reflected energy observed for gold in the low-eV range.[1] It may be that the fraction of the collisions, which cannot be described as binary, increases relatively slowly until the incident energy is reduced to about 20 eV, at which time it begins to increase rather precipitously. This postulate would explains the rather small deviations between experiment and theory observed in the present work and also the previously observed sharp increase in reflected energy starting around 20 eV.

Whereas some of the disagreement between theory and experiment may arise from the inadequacy of the binary-collision model and possibly the method that TRIM.SP uses to correct for nonbinary collisions, it is unlikely that all of it does. This is especially true for the three systems where less energy is reflected than is predicted. The largest disagreement between simulation and experiment is for He-Au, which coincidentally also has the largest mass ratio. Therefore, calculations for He-Au, which use a variety of interaction potentials, electronic stopping formalisms, and screening lengths, are shown in Table VI. Comparison of the experimental data from Table V with the calculations in Table VI shows that experiment does not agree with theory under any conditions. Therefore, it does not seem likely that the input parameters to the TRIM.SP program are the cause for the disagreement between theory and experiment.

Tabata and co-workers have developed empirical formulas for the energy reflection coefficient. Preliminary results are contained in Refs. 29 and 30. The most recent revision of the formulas along with a graphical presentation of the predicted value for the energy-reflection coefficient as a function of incident energy have been compiled for helium in Ref. 3. Comparison of their predicted results with our data shows reasonably good agreement for silver, copper, and carbon. Both our data and the empirical formula indicate less reflected energy for silver than is predicted by the TRIM.SP calculations. However, considering the possible uncertainties in the experiment (2%) and theory (3%–6%), the agreement is not bad. For copper the empirical and TRIM.SP calculations are within experimental uncertainty equal to the experimental results. For carbon the empirical formula, TRIM.SP calculations, and experimental results are all in agreement. For silicon the empirical formula and TRIM.SP calculations are in agreement, while the experimental results indicate more reflected energy than predicted. For gold the predictions of the empirical formula lie between the TRIM.SP calculations and experimental results. It is interesting to note that the empirical formula and experiment are in reasonably close agreement for 4000-eV helium on gold, but digress at lower energy.

Could the data be influenced by surface roughness? This is a difficult question to answer experimentally. Most of the ion-substrate systems reflect more energy than predicted. Multiple scattering due to surface roughness would, however, lead to the opposite behavior. During the course of an experiment, part of the sample is sputtered away. From optical reflectivity measurements it was clear that the sample surface was roughened during the sputtering. Repeating ion-energy-transfer studies under identical conditions for samples that have been exposed to various ion doses showed that the data were reproducible within 2%, i.e., the influence of surface roughness on the experiment is very minor. We, therefore, tentatively conclude that surface roughness does not in general account for the differences between the experi-

TABLE VI. TRIM.SP calculations for energy reflected from gold under bombardment by He^+. Interaction potentials are KR-C (krypton-carbon), Molière, and ZBL (Ziegler, Biersack, and Littmark). The inelastic loss is described by formalisms due to Lindhard and Sharff (LS) and Oen and Robinson (OR). A Firsov screening length (FSL) is used. $R(E)$=energy reflection coefficient, $R(N)$=particle reflection coefficient, and $U_s=3.8$ eV.

	Energy (eV)	$R(E)$	$R(N)$
KR-C, 0.5 LS+0.5 OR, FSL			
	50	0.456	0.679
	4000	0.232	0.435
Moliere, 0.5 LR+0.5 OR, FSL			
	50	0.532	0.738
	4000	0.237	0.428
ZBL, 0.5 LS+0.5 OR, FSL			
	50	0.496	0.706
	4000	0.244	0.439
KR-C, OR, FSL			
	50	0.420	0.645
	4000	0.221	0.419
KR-C, OR, FSL			
	50	0.496	0.715
	4000	0.226	0.429
KR-C, 0.5 LS+0.5 OR, 0.8 FSL			
	50	0.392	0.629
	4000	0.200	0.400

mental data and simulation.

Could the data be influenced by ion channeling? Ion bombardment of single-crystal or polycrystalline silicon is expected to produce an amorphous layer at the surface. Therefore, channeling should not be important for this system. It is also probably unimportant for carbon. However, deposition of copper, silver, and gold produces polycrystalline material with preferred orientation. In our opinion it is possible but not probable that channeling influences the data at these small energies.

VI. SUMMARY

This paper gives a comprehensive set of calculated and experimental values for the energy deposited into carbon, silicon, copper, silver, and gold surfaces by He^+, Ar^+, and Xe^+ ions at normal incidence with kinetic energies in the range 100–4000 eV. The dependence of energy deposition upon ion and substrate mass and ion energy is about that expected from previous work. The experimental trends are reproduced by the calculations which suggest that the binary-collision approximation is a reasonable approach for semiquantative estimates. Nevertheless, there are some quantitative differences in the absolute values, particularly at low incident ion energies and large mass ratios. Arguments and data are presented which suggest that the differences between experiment and simulation are not due to input parameters used in the calculations or due to surface roughness influencing the experimental results. It was not possible to demonstrate scaling laws with reduced energy or mass ratio. The scaling laws are probably operative for larger incident energies than those used in these experiments.

ACKNOWLEDGMENTS

The authors gratefully acknowledge the very capable technical assistance of Dean Pearson and Robert Grygier.

---

*On leave from the Institut of Thin Film and Ion Technology, KFA Julich, Germany.

[1]H. F. Winters, H. Coufal, C. T. Rettner, and D. S. Bethune, Phys. Rev. B **41**, 6240 (1990).

[2]H. F. Winters and E. Kay, J. Appl. Phys. **38**, 3928 (1967).

[3]R. Ito, T. Tabata, N. Itoh, K. Morita, T. Kato, and H. Tawara (unpublished).

[4]D. Hildebrandt and R. Manns, Phys. Status Solidi A **38**, K155 (1976).

[5]J. Schou, H. Sorensen, and U. Littmark, J. Nucl. Mater. **76**, 359 (1978).

[6]H. H. Andersen, T. Lenskjaer, G. Sidenius, and H. Sorensen, J. Appl. Phys. **47**, 13 (1976).

[7]N. N. Koborov, V. A. Kurnaev, V. G. Telkovsky, and G. I. Zhabrev, Radiat. Eff. **69**, 135 (1983).

[8]H. H. Andersen, Radiat. Eff. **3**, 51 (1970).

[9]H. H. Andersen, Radiat. Eff. **7**, 179 (1971).

[10]P. Sigmund, Can. J. Phys. **46**, 731 (1968).

[11]W. Eckstein and J. P. Biersack, Z. Phys. A **310**, 1 (1986).

[12]W. Eckstein and J. P. Biersack, Z. Phys. B **63**, 471 (1976).

[13]O. S. Oen and M. T. Robinson, Nucl. Instrum. Methods **132**, 647 (1976).

[14]H. F. Winters and D. Horne, Phys. Rev. B **10**, 55 (1974).

[15]W. R. Gesang, H. Oechsner, and H. Schoof, Nucl. Instrum. Methods **132**, 687 (1976).

[16]W. Eckstein and H. Verbeck, "Data on Light Ion Reflection," Max-Planck Inst. Plasma Phys. Rep. IPP 9/32 (1979).

[17]H. Sorensen, Appl. Phys. Lett. **29**, 148 (1976).

[18]R. A. Langley, J. Bohdansky, W. Eckstein, P. Mioduszewski, J. Roth, E. Taglauer, W. W. Thomas, H. Verbeek, and K. H. Wilson, Nucl. Fusion, Special Issue, p. 12 (1984).

[19]W. Eckstein, Nucl. Fusion (to be published).

[20]R. Behrisch and W. Eckstein, in *Physics Of Plasma Wall Interactions in Controlled Fusion,* edited by D. E. Post and R. Behrisch (Plenum, New York, 1986).

[21]E. S. Mashkova, Radiat. Eff. **54**, 1 (1981).

[22]W. S. Mashkova and V. A. Mochanov, *Medium-Energy Ion Reflection from Solids* (North-Holland, Amsterdam, 1985).

[23]H. Coufal, R. Grygier, D. Horne, and J. Fromm, J. Vac. Sci. Technol. A **5**, 2875 (1987).

[24]W. D. Wilson, L. G. Haggmark, and J. P. Biersack, Phys. Rev. B **15**, 2458 (1977).

[25]J. O'Connor and J. P. Biersack, Nucl. Instrum. Methods B **15**, 14 (1986).

[26]J. Lindhard and M. Scharff, Dan. Vidensk. Selsk. Mat. Fys. Medd. **25**, 15 (1953).

[27]O. Oen and M. T. Robinson, Nucl. Instrum. Methods **132**, 647 (1976).

[28]J. Ziegler, *The Stopping Ranges of Ion in Matter* (Pergamon, New York, 1977), Vol. 4.

[29]T. Tabata, R. Ito, K. Morita, and Y. Itikawa, Jpn. J. Appl. Phys. **20**, 1929 (1981).

[30]K. Morita, T. Tabata, and R. Ito, J. Nucl. Mater. **128**, 681 (1984).